Eur. Phys. J. D **37**, 385–392 (2006)
DOI: 10.1140/epjd/e2005-00330-3

THE EUROPEAN PHYSICAL JOURNAL D

Cross-sections for rotational excitations of C_3H_4 isomers by electron impact

A.R. Lopes[1], M.H.F. Bettega[2], M.T. do N. Varella[1], and M.A.P. Lima[1,a]

[1] Instituto de Física "Gleb Wataghin", Universidade Estadual de Campinas, 13083-970, Campinas, São Paulo, Brazil
[2] Departamento de Física, Universidade Federal do Paraná, Caixa Postal 19044, 81531-990, Curitiba, Paraná, Brazil

Received 21 September 2005 / Received in final form 31 October 2005
Published online 13 December 2005 –

Abstract. We report elastic (rotationally summed) and rotationally resolved cross-sections for scattering of low-energy electrons by the C_3H_4 isomers allene, propyne, and cyclopropene, which belong to the D_{2d}, C_{3v}, and C_{2v} groups, respectively. We employed the Schwinger multichannel method with pseudopotentials at the static-exchange approximation, combined with the adiabatic-nuclei-rotation (ANR) approximation to calculate the rotational excitation cross-sections for energies ranging from 5 to 30 eV. Our rotational resolved cross-sections show the *isomer effect* more strongly related to scattering potentials of different molecular geometries and to transition selection rules than to differences in mass distribution which account for the energy spacing in the rotational spectra of the molecules.

PACS. 34.80.-i Electron scattering – 34.80.Gs Molecular excitation and ionization by electron impact – 34.80.Bm Elastic scattering of electrons by atoms and molecules

1 Introduction

The knowledge of the cross-sections resulting from electron collisions with hydrocarbons is important in a variety of applications as radiation biochemistry, low-temperature processing plasmas and atmospheric and astrophysical phenomena. Recent experimental studies on electron collisions with isomers of some hydrocarbons verified the existence of the *isomer effect*. Szmytkowski and Kwitnewski [1] measured total cross-sections (TCS) for scattering of electrons by the C_3H_4 isomers allene and propyne, and for C_3H_8 (propane). They found that the shape of the TCS for the two isomers are very similar, especially at high energies, and that both present shape resonance's centered around 2.3 eV for allene, and around 3.4 eV for propyne. Although the shape of the TCS are very similar, they present some features at low energies that allow distinguishing the two TCS, which is the *isomer effect*.

Another experimental study on the C_3H_4 isomers allene and propyne has been done by Nakano et al. [2]. They measured vibrational excitation and elastic differential cross-sections for energies from 1.5 eV to 100 eV. They also calculated the differential cross-sections (DCS) using the continuum multiple-scattering (CMS) method, and found good agreement between their calculated and measured results. The *isomer effect* was discussed for different energies through direct comparison of the DCS for allene and propyne, which is most evident at low energies, where the DCS showed to be very different. These results agree with the observations of Szmytkowski and Kwitnewski. Makochekanwa et al. [3] measured total cross-sections for electron and positron scattering for allene and propyne. They have found differences in the position of the resonance and in the magnitude of the cross-sections of the two isomers (*isomer effect*). Szmytkowski and Kwitnewski [4] have also carried out total cross-section measurements for electron collisions with C_4H_6 isomers 1,3-butadiene and 2-butyne, and also with C_4F_6 (hexafluoro-2-butyne) in which they have also discussed the *isomer effect*.

Motivated by these experimental studies, Lopes and co-workers have carried out electron-collision calculations off several hydrocarbons. Lopes and Bettega [5] performed a theoretical study of electron collisions with the isomers of C_3H_4 allene, propyne and cyclopropene. Qualitative agreement was found between their calculated integral cross-sections for allene and propyne and the total cross-sections of Szmytkowski and Kwitnewski, and very good agreement was found between their calculated differential cross-sections and the results of Nakano et al. [2]. They have also discussed the *isomer effect* which they have found to occur for three isomers for energies below 15 eV. Lopes et al. [6] also calculated cross-sections for the isomers of C_4H_6 1,3-butadiene, 2-butyne, and cyclobutene. Qualitative agreement was found between theory and experiment. In another study, Lopes et al. [7] calculated the cross-sections for isomers of C_4H_8 and C_4H_{10} and showed that scaled elastic integral cross-sections of several simple

[a] e-mail: maplima@ifi.unicamp.br

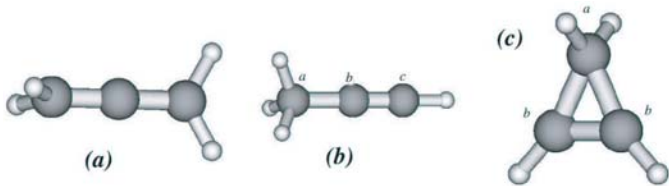

Fig. 1. Geometric structure of (a) allene (D_{2d} symmetry), (b) propyne (C_{3v} symmetry) and (c) cyclopropene (C_{2v} symmetry).

hydrocarbons present similarities. Lopes et al. presented a simple geometric model for this scaling that worked quite well for a whole family of C_nH_m molecules (with combinations of $n = 1, 2, 3, 4$ and $m = 2, 4, 6, 8, 10$), and concluded that all simple hydrocarbons present strong similarities in the cross-sections after the scaling process. Lopes et al. verified that the scaled elastic integral cross-sections for these hydrocarbons coincide at energies from 10–40 eV, and also that the geometry of the molecule has little effect for low energy scattering at the static-exchange approximation. In general, in these former articles the *isomer effect* due to charge distribution have been exploited. Now, to improve the understanding of the *isomer effect* we present in this paper our calculated rotationally elastic and inelastic cross-sections for electron impact of the isomers allene, propyne and cyclopropene.

Our results were obtained using the Schwinger multichannel method with pseudopotentials (SMCPP), in the static-exchange approximation, combined with the adiabatic-nuclei-rotation (ANR) approximation [8]. The C_3H_4 isomers, allene, propyne and cyclopropene, belong to the D_{2d}, C_{3v}, and C_{2v} symmetry groups, respectively. We report state-to-state cross-sections, departing from the rotational ground state of the target ($J = 0 \rightarrow J' = 0$, 1, 2, 3, 4, 5, 6). Such state-to-state cross-sections are the fundamental information concerning pure rotational energy transfer in gaseous discharges. Pure rotational energy transfer from electrons to molecular gases in slow collisions is often quite effective. Even though the energy transfer per collision is quite small for polyatomic molecules, the cross-sections may be very large ($\sim 10^{-16}$ cm^2). As a result, either in gas discharges or in the ionosphere of the Earth, a considerable fraction of the total energy of the free-electron gas is transferred to the rotational energy of molecules.

The geometric structures of the C_3H_4 isomers are shown in Figure 1. To generate this figure we used the packages GAMESS [9] and Molden [10]. The isomer allene ($H_2C{=}C{=}CH_2$) has two double bonds, propyne ($HC{\equiv}C{-}CH_3$) has triple and single bonds and are open-chain (with linear carbon chains) hydrocarbons with different C−C bond multiplicity. These isomers are symmetric-top molecules. The isomer cyclopropene ($CH{-}CH_2{-}CH$) is a closed-chain hydrocarbon and has one double bond and two single bonds, and is an asymmetric-top molecule.

In the next sections we present a brief description of the theoretical formulation of our method, the computational procedures used in our calculations, our results and discussion, as well as a brief summary of our findings.

2 Theory

The SMC method [11–13] and its implementation with pseudopotentials (SMCPP) [14] have been previously described in detail, and we will only outline a few aspects relevant to the present work. The resulting expression for the scattering amplitude is given by

$$f(\vec{k}_f, \vec{k}_i) = -\frac{1}{2\pi} \sum_{m,n} \langle S_{\vec{k}_f} | V | \chi_m \rangle (d^{-1})_{mn} \langle \chi_n | V | S_{\vec{k}_i} \rangle \quad (1)$$

where

$$d_{mn} = \langle \chi_m | A^{(+)} | \chi_n \rangle \quad (2)$$

and

$$A^{(+)} = \frac{\hat{H}}{N+1} - \frac{(\hat{H}P + P\hat{H})}{2} + \frac{(VP + PV)}{2} - VG_P^{(+)}V. \quad (3)$$

In the above equations, $|S_{\vec{k}_{i,f}}\rangle$ is a solution of the unperturbed Hamiltonian H_0 and is a product of a target state and a plane wave, V is the interaction potential between the incident electron and the electrons and nuclei of the target, $|\chi_m\rangle$ is a set of $(N+1)$-electron Slater determinants (Configuration State Functions-CSF's) used in the expansion of the trial scattering wave function, $\hat{H} = E - H$ is the total energy of the collision minus the full Hamiltonian of the system, with $H = H_0 + V$, P is a projection operator onto the open-channel space defined by the target eigenfunctions, and $G_P^{(+)}$ is the free-particle Green's function projected on the P-space. The (direct) configuration space is constructed as:

$$\{|\chi_i\rangle\} = \{\mathcal{A}\,(|\Phi_1\rangle \otimes |\varphi_i\rangle)\} \quad (4)$$

where $|\Phi_1\rangle$ is the target ground state wave function, described at the Hartree-Fock level of approximation, $|\varphi_i\rangle$ is a one-electron function, and $\mathcal{A}$ is the antisymmetrizer.

The ANR approximation expression for the rotational excitation scattering amplitude is given by [8]

$$f_{\Gamma \rightarrow \Gamma'} = \langle \Psi^*_{\Gamma'} | f^{elas}(k_{in}, \mathbf{k}_{out}, \Omega) | \Psi_\Gamma \rangle, \quad (5)$$

where Ψ_Γ is a target rotational eigenfunction (Γ denotes a complete set of rotational quantum numbers), $\Omega \equiv (\alpha, \beta, \gamma)$ are the Euler angles defining the transformation from the body–fixed frame (BF) to the laboratory–fixed frame (LF), and f^{elas} is the elastic scattering amplitude, presently obtained with the SMCPP method (Eq. (1)). For symmetric tops, such as allene and propyne, the rotational eigenfunctions are related to the Wigner rotation matrices [15]

$$\Psi_{JKM}(\Omega) = \left(\frac{2J+1}{8\pi^2}\right)^{\frac{1}{2}} D^{J*}_{KM}(\Omega), \quad (6)$$

where J is the molecular angular momentum, and K and M are the projections onto the quantization axes of the BF and LF, respectively. Symmetric tops have $2(2J+1)$–fold degenerate energy levels,

$$E_{JK} = BJ(J+1) + (A-B)K^2, \tag{7}$$

where the rotational constants A and B are related to the molecular moments of inertia (I_{xx}, I_{yy}, I_{zz}) according to $B = (1/2I_{xx} + 1/2I_{yy} + 1/2I_{zz})$ and $A = 1/2I_{zz}$. For asymmetric tops (cyclopropene), K is no longer a good quantum number and the rotational eigenfunctions may be written as symmetry–adapted combinations of symmetric–top eigenfunctions [16]

$$\Psi^s_{J\tau M}(\Omega) = \sum_{K=0}^{J} \sum_{\nu=0}^{1} a^{J\tau}_{KM} \phi^{s\nu}_{JKM}(\Omega), \tag{8}$$

with

$$\phi^{s\nu}_{JKM}(\Omega) = \frac{1}{\sqrt{2}} \left[\Psi_{JKM} + (-1)^\nu \Psi_{J-KM}\right]; \quad K > 0,\ \nu = 0, 1, \tag{9}$$

and

$$\phi^{s\nu}_{JKM}(\Omega) = \Psi_{JKM}\delta_{\nu 0}; \quad K = 0, \tag{10}$$

where τ is a pseudoquantum number labeling the eigenstates. The procedure to diagonalize the rotational Hamiltonian of an asymmetric top, thus obtaining the $a^{J\tau}_{KM}$ coefficients and the corresponding energy levels, is discussed elsewhere [16].

The rotational excitation cross-section can be written as

$$\frac{d\sigma}{d\Omega}(JN \to J'N', \theta'_{out}) = \frac{1}{2\pi} \frac{1}{(2J+1)} \times \sum_{M=-J}^{J} \sum_{M'=-J'}^{J'} \frac{k_{j'N'}}{k_{jN}} \int d\phi |f(JNM \to J'N'M')|^2, \tag{11}$$

where $N = K$ for symmetric tops and $N = \tau$ for asymmetric tops. Finally, we observe that scattering amplitudes calculated in the BF may be written in the LF through the usual transformation of spherical harmonics [15],

$$f^{elas}_{\rm LF}(k_{in}, \mathbf{k}_{out}, \Omega) = \sum_{lm} f^{\rm LF}_{lm}(k_{in}, \Omega)\, Y_{lm}(\hat{\mathbf{k}}_{out}), \tag{12}$$

with

$$f^{\rm LF}_{lm}(k_{in}, \Omega) = \sum_{\mu} D^l_{m\mu}(-\gamma, -\beta, -\alpha)\, f^{\rm BF}_{l\mu}(k_{in}, \beta, \alpha), \tag{13}$$

where we have used the relation between the incident direction in the BF and the Euler angles, $\hat{\mathbf{k}}_{in} = (\beta, \alpha)$.

Table 1. Rotational constants of C_3H_4 isomers.

isomer	constants (cm^{-1})		
	A	B	C
allene	4.854	0.297	–
propyne	5.322	0.285	–
cyclopropene	1.004	0.729	0.461

Table 2. Dipole moments (D) for the C_3H_4 isomers.

System	calc.	exp.
propyne	0.807	0.784 ([18])
allene	0.000	–
cyclopropene	0.509	0.450 ([18])

3 Computational details

Our calculations were performed with the Schwinger multichannel method along with the pseudopotentials of Bachelet, Hamann, and Schlüter [17], at the fixed-nuclei and static-exchange approximation combined with the ANR approximation. We used the ground state equilibrium geometries of allene, propyne, and cyclopropene given in reference [18], and the corresponding rotational constants are given in Table 1. The basis set for the carbon atom is formed by 6 uncontracted s-type functions (with exponents 12.49408, 2.470291, 0.614027, 0.184029, 0.036799, and 0.013682), 5 uncontracted p-type functions (with exponents 5.228869, 1.592058, 0.568612, 0.210326, and 0.072250), and 2 uncontracted d-type functions (with exponents 0.603592, and 0.156753), and was generated according reference [19]. The basis set for the hydrogen atom are in reference [5]. The partial-wave decomposition of the elastic scattering amplitudes were truncated at $\ell = 10$. The rotationally summed cross-sections have included all excitations up to $J = 6$.

The calculated and experimental dipole moments for the C_3H_4 isomers are shown in Table 2. In previous studies of polar targets [20] we employed a correction to account for the long-ranged interaction due to permanent dipole moments. Such corrections are not expected to be important here, in view of (i) the modest magnitude of the dipole moments, and (ii) the large impact parameters arising from the size of the targets and from the addressed energy range (above 5 eV). The resulting dipole-moment corrections would only contribute to differential cross-sections of the dipole-allowed transitions ($00 \to 10$) at very low scattering angles, and may be safely neglected. Since polarization is expected to be important around 5 eV and below [5], the static-exchange approximation should provide reliable results in the present study.

4 Results and discussion

In Figure 2 we show the rotationally summed and rotationally unresolved [5] integral cross-sections for allene (upper panel), propyne (central panel) and cyclopropene

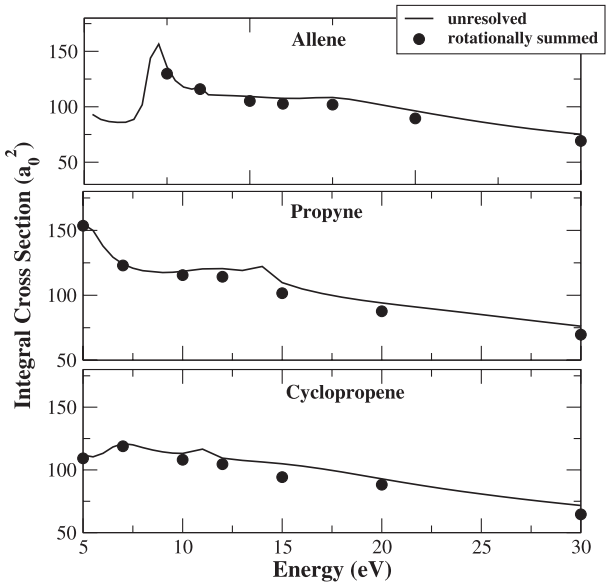

Fig. 2. Integral cross-section for C_3H_4 isomers. Solid line: elastic (rotationally unresolved); circles: rotationally summed.

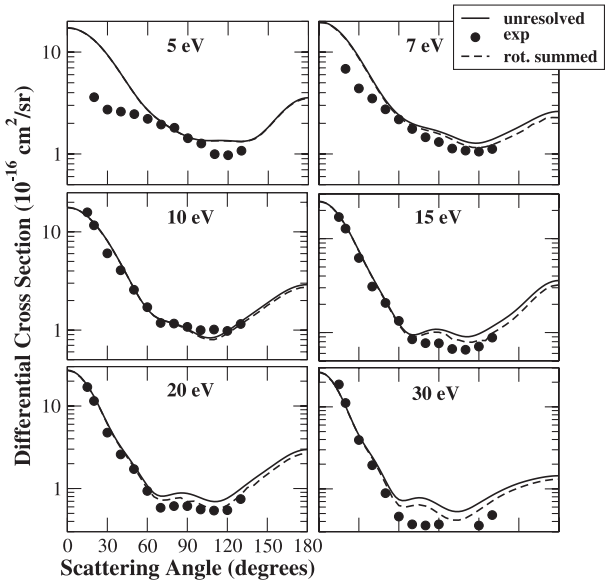

Fig. 3. Differential cross-section for allene. Solid line: elastic (rotationally unresolved); dashed line: rotationally summed; circles: experimental data of Nakano et al. [2].

(lower panel) for energies from 5 eV up to 30 eV. For the three isomers we have summed rotational excitation cross-sections for the $J = 0 \rightarrow J' = 0, 1, 2, 3, 4, 5, 6$ transitions. The rotationally summed cross-section presents a very good convergence, though differences of a few percent become evident at higher energies, where transitions to higher angular momenta become more effective.

To illustrate the agreement between theory and experiment, in Figure 3 we compare the elastic differential cross-sections (rotationally unresolved) with the rotationally summed cross-sections for allene and with the experimental results of Nakano et al. [2] at 5, 7, 10, 15, 20 and 30 eV. Again, comparison between elastic and rotationally summed differential cross-sections indicates very good convergence of the latter. The small discrepancy at high scattering angles is due to the truncation of the sum at $J = 6$, being more noticeable beyond 20 eV.

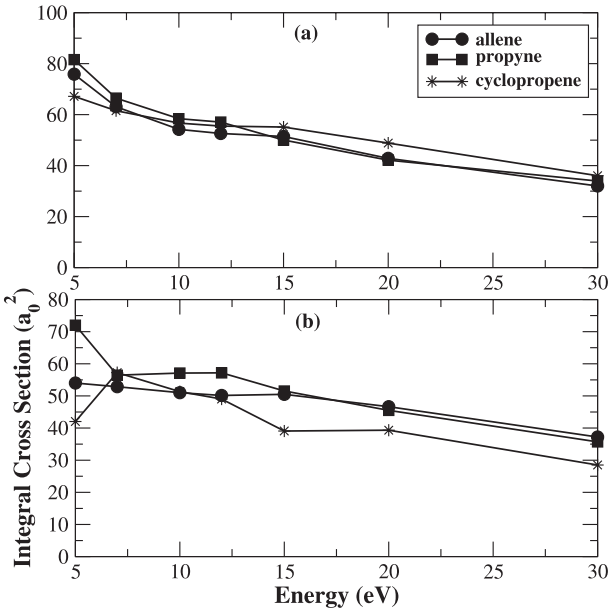

Fig. 4. Integral cross-sections for C_3H_4 isomers. (a) Rotationally elastic cross-sections and (b) rotationally summed inelastic cross-sections. Solid line with circles: allene; solid line with squares: propyne; solid line with stars: cyclopropene.

In the upper panel of Figure 4 we show the rotationally elastic cross-sections ($00 \rightarrow 00$) for allene, propyne and cyclopropene. Although the cross-sections are similar, specially in shape, there is a crossing point around 12.5 eV where the ordering of cross-section magnitudes changes from $\sigma_{allene} > \sigma_{propyne} > \sigma_{cyclopropene}$ to $\sigma_{allene} < \sigma_{propyne} < \sigma_{cyclopropene}$. In the lower panel we show inelastic rotationally summed cross-sections for the three isomers. The inelastic cross-section of cyclopropene is quite different from those of the other two isomers. For allene and propyne, the cross-sections differ below 15 eV and become very similar above 15 eV. The *isomer effect* is more evident for cyclopropene, probably due to the different geometry (closed chain) of the carbon atoms, more efficient scatters than hydrogen atoms.

In Figure 5 we show the differential rotationally summed inelastic cross-sections for the C_3H_4 isomers at 5, 7, 10, 15, 20 and 30 eV. The three isomers can be identified from the respective cross-sections, though allene and propyne have similar shapes. At 20 and 30 eV, allene and propyne show a broad structure around 40°, not present in cyclopropene results. In general, cyclopropene cross-sections are easily distinguishable for collision energies other than 10 eV. Figure 6 shows the cross-sections for the $00 \rightarrow 00$ transition (rotationally elastic) at 5, 7, 10, 15, 20 and 30 eV. At low energies, results for the three isomers are markedly different. Cyclopropene presents a minimum around 70° at 7 eV and the second minimum

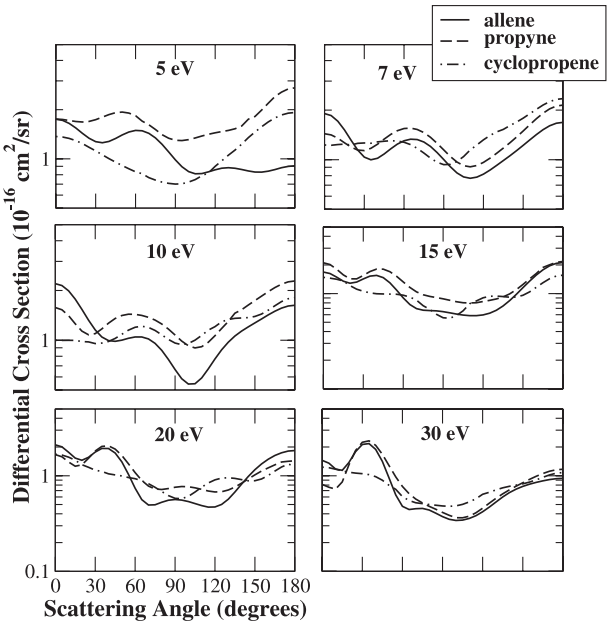

Fig. 5. Differential rotationally summed inelastic cross-section at 5, 7, 10, 15, 20 and 30 eV for allene (solid line), propyne (dashed line) and cyclopropene (dot–dashed line).

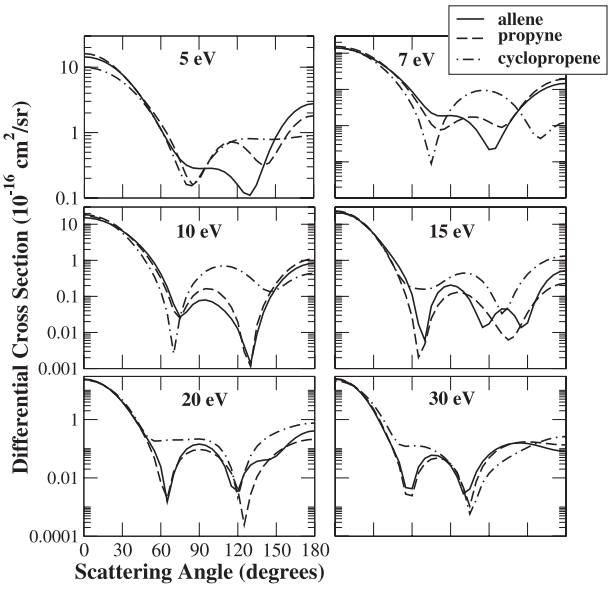

Fig. 6. Differential rotationally elastic cross-section (00 → 00) at 5, 7, 10, 15, 20 and 30 eV for allene (solid line), propyne (dashed line) and cyclopropene (dot–dashed line).

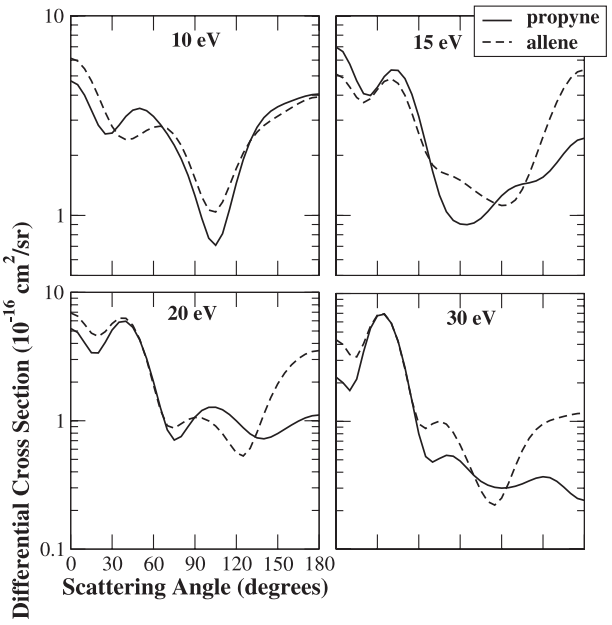

Fig. 7. Differential cross-section for the rotational excitation 00 → 20 for propyne (solid line) and allene (dashed line) at 10, 15, 20 and 30 eV.

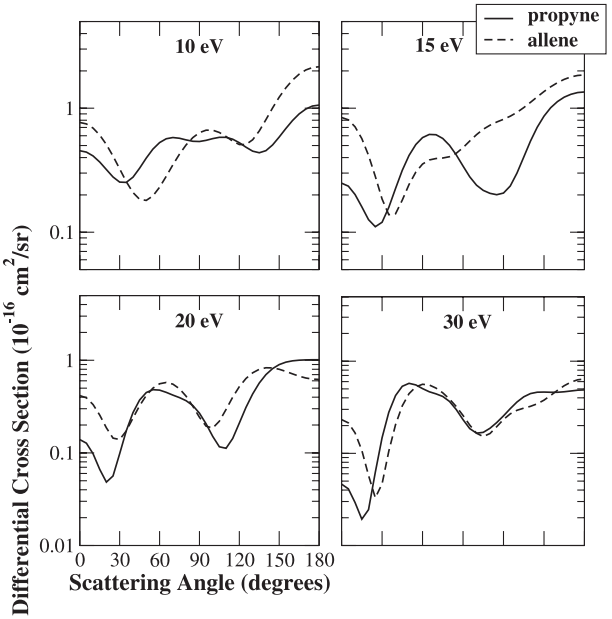

Fig. 8. Differential cross-section for the rotational excitation 00 → 40 for propyne (solid line) and allene (dashed line) at 10, 15, 20 and 30 eV.

around 150° at 10 eV, while allene and propyne present the second minima around 120° (10 eV). At 15 eV calculations for allene show three minima while only two minima for propyne and cyclopropene, thus suggesting a strong *isomer effect* in the rotationally elastic cross-section. Finally, cyclopropene presents only one minimum at 30 eV, while the open–chain isomers have very similar cross-sections.

In general, allene and propyne often have similar cross-sections differing from those of the cyclic isomer. As long as rotational excitations are concerned, such differences would be expected to follow from mass distributions, since cyclopropene is an asymmetric top (the other isomers are symmetric tops). Hence, it would be interesting to investigate differences between the two open–chain molecules, and we show in Figures 7, 8, and 9 the differential cross-sections for the 00 → 20, 40 and 60 excitations at 10, 15, 20 and 30 eV. In all cases, there are differences in magnitude, though a crossing around 20° is noticed in the 00 → 40 cross-sections (Fig. 8). Note also that allene presents more

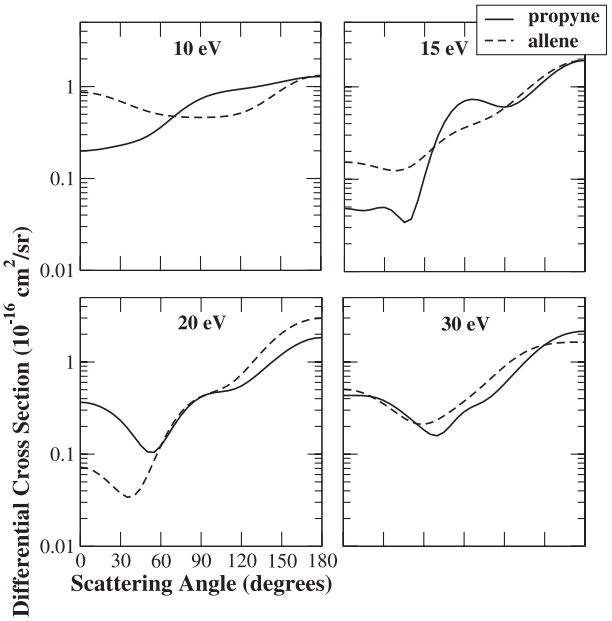

Fig. 9. Differential cross-section for the rotational excitation $00 \rightarrow 60$ for propyne (solid line) and allene (dashed line) at 10, 15, 20 and 30 eV.

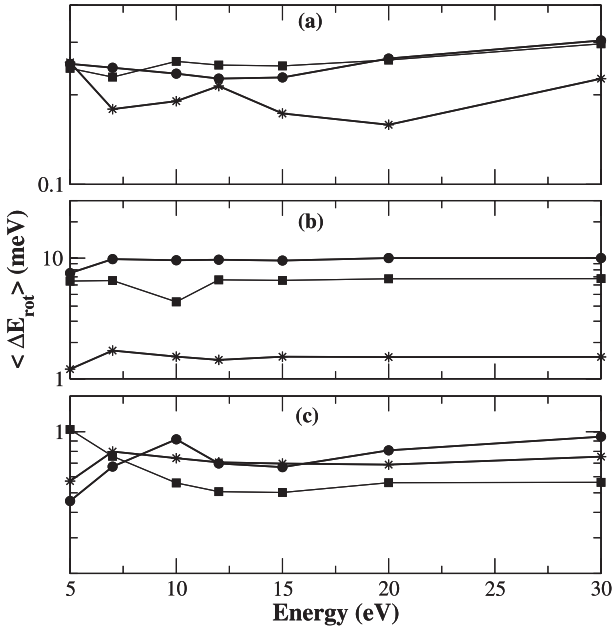

Fig. 10. Computed average rotational energy transfer for allene (circles), propyne (squares) and cyclopropene (stars).

pronounced minima around 120° at 20 and 30 eV, while rather similar shapes are found at lower collision energies.

An useful indicator of the relative efficiency of rotationally inelastic collisions is given by the evaluation, out of a selected rotational level of the target molecule, of an average energy transfer index defined as [21]

$$\langle \Delta E_{rot} \rangle_{JN} = \frac{\sum_{J'N'} \sigma_{JN \rightarrow J'N'} \Delta\varepsilon_{JNJ'N'}}{\sum_{J'N'} \sigma_{JN \rightarrow J'N'}} \qquad (14)$$

where JN labels the rotational states ($N \equiv K$ for symmetric tops and $N \equiv \tau$ for asymmetric tops), and $\Delta\varepsilon_{JNJ'N'}$ is the corresponding rotational energy transfer. The low–energy behavior of $\langle \Delta E_{rot} \rangle_{00}$ for allene, propyne and cyclopropene is shown in Figure 10, where the sum over final states runs from $J' = 0$ to 6. In the upper panel of Figure 10, only transitions to $N' = 0$ are taken into account, while only transitions to $N' \neq 0$ in the central panel, and all possible N' values in the lower panel. As expected, cyclopropene differs from the open-chain isomers, though it should be noted that allene and propyne show an evident *isomer effect* in the rotational-energy-transfer efficiency over the whole range of impact energies, especially for those transitions with $K \neq 0$. In principle, this may be due to the symmetry of the scattering potential (charge distribution) and the underlying selection rules for rotational excitations, or to the average spacing between rotational levels (mass distribution). The rotational constants in Table 1 suggest that mass effects should be more noticeable in transitions with $K \neq 0$ (see also Eq. (7)), because $B_{\text{allene}} \simeq B_{\text{propyne}}$ while $(A - B)_{\text{allene}} < (A - B)_{\text{propyne}}$. This simple argument would lead to the conclusion that $\langle \Delta E \rangle_{\text{allene}} < \langle \Delta E \rangle_{\text{propyne}}$, but the opposite is noted in

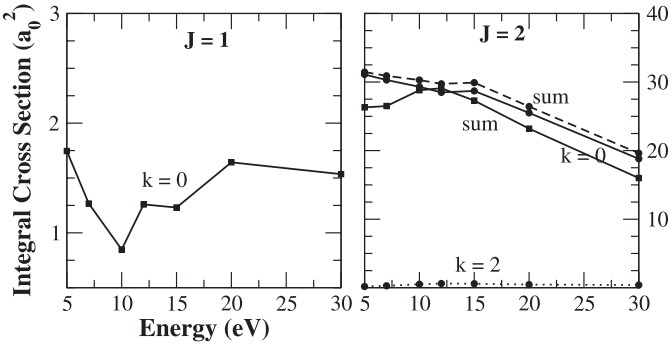

Fig. 11. Rotationally inelastic cross-sections for allene and propyne. Each insert contains a given rotational excitation exit channel ($J = 1, 2$) and all K values with non-zero contribution. Rotationally summed inelastic cross-sections for each J value are also shown, when more than one K value contributes. Allene: full circles; propyne: full squares.

Figure 10, thus indicating that charge and symmetry effects should actually prevail. To better understand the origin of these effects, Figures 11, 12 and 13 show rotationally resolved cross-sections for given values of J and different values of K for allene and propyne isomers. Only the contributing exit channels are shown and the *isomer effect* can be clearly noticed in these figures. It is interesting to note, however, that for some of the angular momentum J, if we sum all K contributions, the *isomer effect* can be disguised. Through the analysis of these resolved cross-sections, it is possible to realize that the selection rules can strongly influence the capacity of a molecule to receive rotational energy by electron impact. Finally Figure 14 shows the average energy transfer calculated for allene and propyne with exchanged rotational constants.

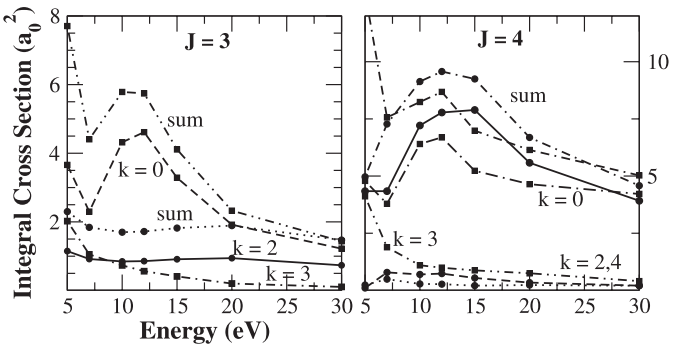

Fig. 12. Same as Figure 11 for $J = 3, 4$.

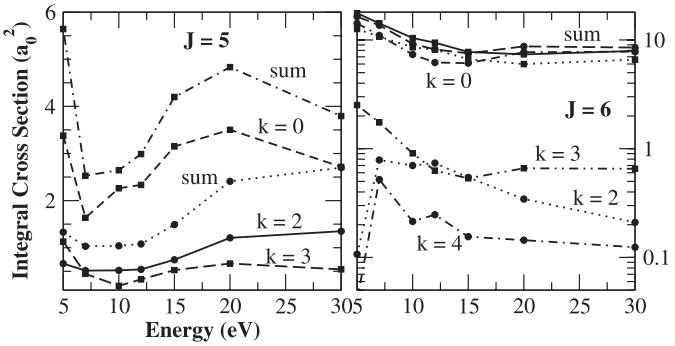

Fig. 13. Same as Figure 11 for $J = 5, 6$.

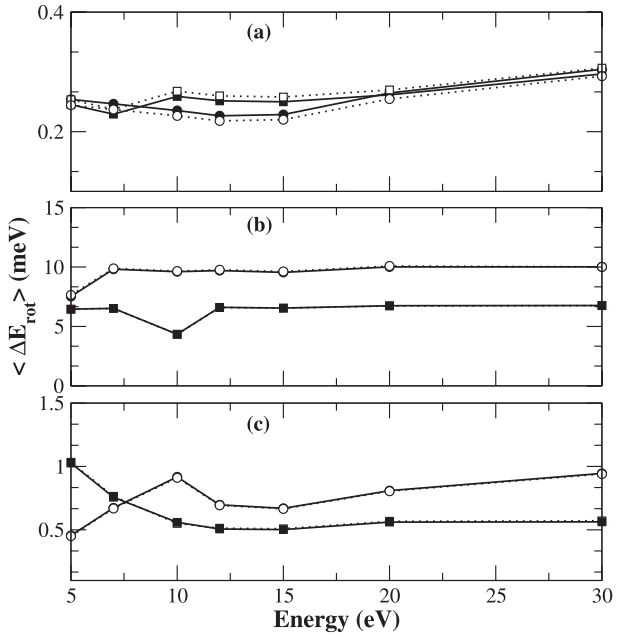

Fig. 14. Computed average rotational energy transfer for allene (circles) and propyne (squares). The solid lines with filled symbols are the same as in Figure 10, while dashed lines with hollow symbols were obtained with exchanged rotational constants (see text).

The effect of this exchange is switching the mass distribution of the two molecules, i.e., inserting the mass distribution of allene into propyne and vice-versa. A relatively small change is introduced, indicating that the *isomer effect* is indeed related to the differences in the scattering potentials (charge distribution) and selection rules of the molecules.

5 Summary

We presented elastic (rotationally summed) and rotationally inelastic differential and integral cross-sections for scattering of low-energy electrons by C_3H_4 isomers, allene, propyne, and cyclopropene. The results show the existence of *isomer effect* due to different molecular charge distributions which are more evident for cyclopropene (closed chain). For allene and propyne, such effects become more evident in state–to–state rotational excitation cross-sections. We have also learned that different transition selection rules of the isomers strongly influence the efficiencies of rotational energy transfer, thus allowing distinction of the three isomers through their ability to warm up (rotationally) by electron impact.

ARL and MTNV acknowledge scholarships from Fundação de Amparo à Pesquisa do Estado de São Paulo (Fapesp). MHFB and MAPL acknowledge support from Brazilian agency Conselho Nacional de Desenvolvimento Científico e Tecnológico (CNPq). MHFB acknowledges support from the Paraná state agency Fundação Araucária, from FINEP (under project CT-Infra 1), and also computational support from Prof. Carlos M. de Carvalho at Departamento de Física–UFPR. The calculations were carried out at CENAPAD–SP and DF–UFPR. The authors acknowledge Prof. Luiz G. Ferreira for enlightening discussion on effects of mass distribution in quantum mechanics.

References

1. C. Szmytkowski, S. Kwitnewski, J. Phys. B: At. Mol. Opt. Phys. **35**, 3781 (2002)
2. Y. Nakano, M. Hoshino, M. Kitajima, H. Tanaka, M. Kimura, Phys. Rev. A **66**, 032714 (2002)
3. C. Makochekanwa, H. Kawate, O. Sueoka, M. Kimura, M. Kitajima, M. Hoshino, H. Tanaka, Chem. Phys. Lett. **368**, 82 (2003)
4. C. Szmytkowski, S. Kwitnewski, J. Phys. B: At. Mol. Opt. Phys. **36**, 2129 (2003)
5. A.R. Lopes, M.H.F. Bettega, Phys. Rev. **67**, 32711 (2003)
6. A.R. Lopes, M.A.P. Lima, L.G. Ferreira, M.H.F. Bettega, Phys. Rev. A **69**, 014702 (2004)
7. A.R. Lopes, M.H.F. Bettega, M.A.P. Lima, L.G. Ferreira, J. Phys. B **37**, 997 (2004)
8. D.M. Chase, Phys. Rev. **104**, 838 (1956)
9. M.W. Schmidt, K.K. Baldridge, J.A. Boatz, S.T. Elbert, M.S. Gordon, J.H. Jensen, S. Koseki, N. Matsunaga, K.A. Nguyen, S.J. Su, T.L. Windus, M. Dupuis, J.A. Montgomery, J. Comput. Chem. **14**, 1347 (1993)

10. G. Schaftenaar, J.H. Noordik, J. Comput.-Aided Mol. Des. **14**, 123 (2000)
11. K. Takatsuka, V. McKoy, Phys. Rev. A **24**, 2473 (1981)
12. K. Takatsuka, V. McKoy, Phys. Rev. A **30**, 1734 (1984)
13. M.A.P. Lima, L.M. Brescansin, A.J.R. da Silva, C. Winstead, V. McKoy, Phys. Rev. A **41**, 327 (1990)
14. M.H.F. Bettega, L.G. Ferreira, M.A.P. Lima, Phys. Rev. A **47**, 1111 (1993)
15. M.E. Rose, *Elementary Theory of Angular Momentum* (John Wiley and Sons, New York, 1957)
16. C. Van Winter, Physica **20**, 274 (1954); A. Jain, D.G. Thompson, Comput. Phys. Commun. **30**, 301 (1983)
17. G.B. Bachelet, D.R. Hamann, M. Schlüter, Phys. Rev. B **26**, 4199 (1982)
18. *CRC Handbook of Chemistry and Physics*, 79th edn., edited by D.R. Lide (CRC, Boca Raton, 1998)
19. M.H.F. Bettega, A.P.P. Natalense, M.A.P. Lima, L.G. Ferreira, Int. J. Quant. Chem. **60**, 821 (1996)
20. M.T. do N. Varella, M.H.F. Bettega, A.J.R. da Silva, M.A. P. Lima, J. Chem. Phys. **110**, 2452 (1999); M.T. do N. Varella, M.H.F. Bettega, M.A.P. Lima, L.G. Ferreira, J. Chem. Phys. **111**, 6396 (1999); A.P.P. Natalense, M.T. do N. Varella, M.H.F. Bettega, L.G. Ferreira, M.A.P. Lima, J. Phys. B: At. Mol. Opt. Phys. **32**, 5523 (1999)
21. F.A. Gianturco, T. Mukherjee, P. Paioletti, Phys. Rev. A **56**, 3638 (1997); F.A. Gianturco, T. Stoecklin, Phys. Rev. A **55**, 1937 (1997); S. Telega, E. Bodo, F.A. Gianturco, Eur. Phys. J. D **29**, 357 (2004)